

Initial Electron Beam Polarization Measurement in $e\text{-}\gamma$ Collisions

Gökhan ÜNEL

*Department of Physics and Astronomy, Northwestern University,
Evanston, IL 60208, U.S.A.*

Received 17.03.2003

Abstract

The future high energy ee colliders, together with the complementary $\gamma\gamma$ option, will offer possibilities for both discovery and precision physics. The uncertainty on the initial beam polarizations contributes to the systematic errors in each case. Therefore, it is crucial to obtain the precise beam polarizations by independent measurements. The $e\gamma \rightarrow \nu W$ process in the $e\gamma$ mode can be used to experimentally determine the polarization of the initial e beam. This note addresses the feasibility of making such a measurement with a relative statistical error of one percent. Generator and detector level MC tools are used to obtain a realistic simulation of the signal and background processes at the future CLIC test facility running at $\sqrt{s} = 150$ GeV. We estimate about 8 months of data collection time by combining the muon and electron channels.

Key Words: Linear Collider, Laser backscattering, Beam polarization, Simulation, CLIC

1. Introduction

The next high energy ee colliders [1] or their predecessor test facilities will be capable of achieving highly polarized $\gamma\gamma$ and $e\gamma$ collisions at high luminosities due to recent advancements in laser technology [2]. In the $e\text{-}\gamma$ collisions, which can uniquely be identified due to the net -1 charge in the final state, a very interesting process is

$$e^- \gamma \rightarrow \nu_e W^-. \quad (1)$$

Depending on the center of mass energy \mathcal{E} , the luminosity \mathcal{L} of the collider and the polarization \mathcal{P} of the beams, this process can be used to investigate the anomalous trilinear gauge boson couplings at high energy with polarized beams [3], the leptoquarks and the composite charged gauge bosons [4], and to provide ways to determine the value of the beam polarization at high \mathcal{L} [5].

The initial electron beam polarization will contribute to the systematic error on any measurement and will thus be a limiting factor on the total error. This note, therefore, focuses on the measurement of the initial electron beam polarization with a small relative error of about 1 percent. After putting down the requirements on the polarization measurement, the properties of the signal process and the source for the direct background events will be presented. The second section summarizes the Monte Carlo tools used during this study. The results for event selection efficiency and background rejection will be shown for different final states in section three. Finally, data collection time estimates for the intended electron polarization measurement in the proposed CLIC1 [5] accelerator, are obtained using different W^- decay channels. Since CLIC1 will solely be an electron accelerator, the positron beam is not considered in this work.

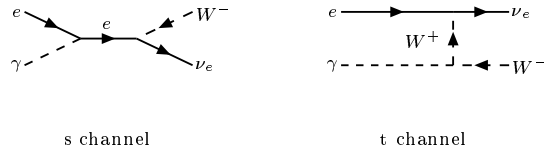


Figure 1. Channels yielding the $\nu_e W^-$ final state in $e\gamma$ collisions.

The lowest order Feynman diagrams that would yield a $\nu_e W^-$ final state are shown in Figure 1. In the Standard Model, with massless neutrinos, the helicity of the incoming e^- is fixed by the ν_e , implying zero contribution to the total cross section σ_T from the right handed electrons e_R . Therefore the s channel diagram can even be turned off by choosing 100% opposite e^- and γ polarizations. This concept will be the key point to measure the beam polarization. The surviving t channel diagram is of particular interest since the trilinear gauge boson coupling allows testing, among other things, the V-A structure of the standard model [6], and the extra charged gauge bosons [7].

If one assumes a fixed laser photon beam polarization, the change in the total cross section of the signal process due to the change in electron beam polarization can be computed as shown in Figure 2. We note that in order to determine the electron polarization with an error of 1.0%, one has to measure the cross section with an accuracy of 5 permille. For the estimation of the required data taking time for such a measurement, only statistical errors and direct backgrounds will be considered. The contributions from the misidentifications and other systematic errors are detector dependent and, therefore, they are not included in this work.

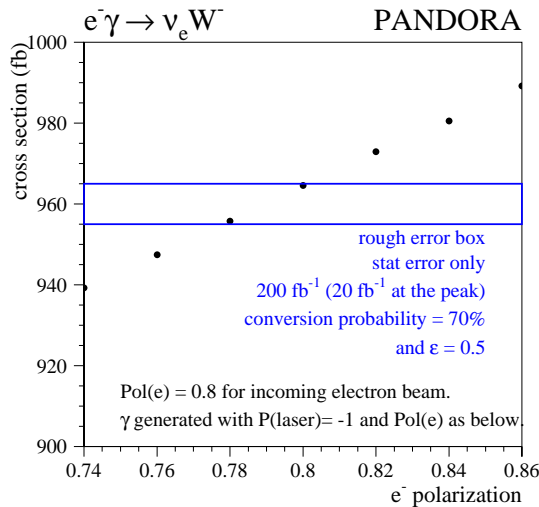


Figure 2. Cross section of the signal process as a function of the electron polarization as obtained from Pandora. [5].

Naturally, the $W^- \nu_e$ final state will be identified through W^- 's decay products. The possible tree level background to the final states will arise from the photon structure [8] and invisible Z decays. Figure 3 shows the background diagrams coming from the leptonic and hadronic structure of the photon for the decay channels not containing electrons. Figure 4 contains the background diagrams for the electron final states including the additional backgrounds from the the invisible decays of the Z boson.

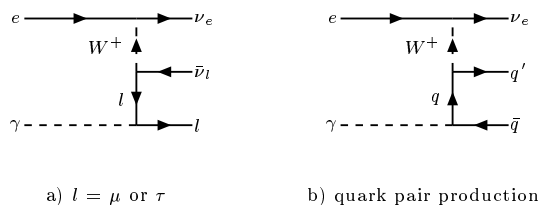


Figure 3. Possible background processes for μ, τ and hadronic decays of W^- .

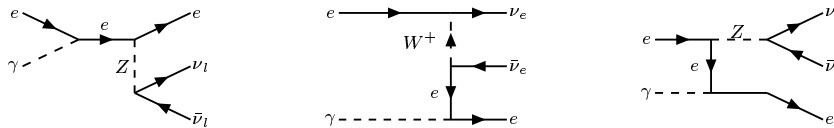


Figure 4. Possible background processes for e^- decay of W^- .

2. MC tools and Backgrounds

To simulate the signal and background processes, two different event generators are considered:

Pandora V2.21 This is a tree-level generator which takes into account the beam polarization [9]. This version can only calculate $2 \rightarrow 2$ processes. The generated events can be fed into Pythia (v6.128) [10] for fragmentation through the `pandora-pythia` interface [11].

CompHEP V41.10 This is also a tree level generator [12]. CompHEP is for unpolarized electron beams only, but it can simulate $2 \rightarrow 3$ processes, which are crucial for the study of backgrounds. The interface to Pythia (v6.128) for fragmentation is `cpyth` [13].

The simulations presented in this note are solely from CompHEP, since Pandora can't be used to compute the backgrounds. Although CompHEP has only unpolarized beams, the case of 100% opposite electron and photon helicities in the signal process can be simulated by artificially turning off the s channel in Figure 1. The beamline parameters can be tuned in both generators for realistic beamstrahlung estimation. For the computations in this note, the proposed CLIC Higgs Experiment's parameters (based on CLIC1 Test Facility) are used [5]: bunch size $(x + y) = 157$ nm, bunch length = 0.03 mm, $N_e/\text{bunch} = 4 \times 10^9$. The photon spectrum in both generators is pure laser spectrum, without the Williams Weizsacker [14] contribution. For Pandora, the laser is taken to be 100% polarized.

The parameter x , commonly known as Telnov's x [15], is used to relate the maximum photon energy E_γ to the energies of the initial electron beam E_e and the laser beam w , and are expressed as:

$$\begin{aligned} x &\equiv \frac{4E_e w}{m_e^2}, \\ E_\gamma &= \frac{x}{x+1} E_e. \end{aligned} \quad (2)$$

A Higgs particle of mass about 120 GeV [16], requires the optimization of the photon beams in the planned CLIC1 machine with \mathcal{E}_{ee} of 150 GeV. Therefore, the value of x becomes $x = 4.0507$, different than the conventional value of 4.83 [1]. To get a converging value for the cross section, a minimum set of cuts are applied at the generator level:

$$\begin{aligned} P_T(W^-) &> 5 \text{ GeV}, \\ E_{cm} &> 2 \text{ GeV}, \\ \Theta &> 1^\circ, \end{aligned}$$

where P_T is the transverse momentum of the W , E_{cm} is the center of mass energy of the $W^- \nu_e$ pair and Θ is the azimuthal angle of the W^- relative to the beam pipe. Since the original study in Figure 2 was done with Pandora, and this note uses CompHEP exclusively, it is necessary to show their mutual agreement on the signal process. The total effective cross sections ($\sigma \times \text{Br}$, after cuts) obtained from both generators using unpolarized electron beams are :

$$\begin{aligned} \sigma(\text{CompHEP}) &= 2661 \pm 2 \text{ fb}, \\ \sigma(\text{Pandora}) &= 2495 \pm 2 \text{ fb}. \end{aligned}$$

The small difference in the cross sections is understandable in light of the slight difference in the peak position of the laser backscattered photon spectra of Figure 5. After fragmentation, both generators give

Table 1. Cross section×Branching ratio (in fb) of signal and background processes for the leptonic decays of W^- from CompHEP.

channel	$\sigma_{signal} \times Br$ (fb)	$\sigma_{backg.} \times Br$ (fb)
$e \gamma \rightarrow \nu W, (W^- \rightarrow \tau \bar{\nu}_\tau)$	276.0 ± 1.24	35.68 ± 0.08
$e \gamma \rightarrow \nu W, (W^- \rightarrow \mu \bar{\nu}_\mu)$	276.1 ± 1.65	36.44 ± 0.09
$e \gamma \rightarrow \nu W, (W^- \rightarrow e \bar{\nu}_e)$	276.8 ± 1.9	1116 ± 4

outputs in StdHEP format which are then processed by the fast simulation program of an NLC type detector. For this analysis a generic “small detector” is selected. The description of the fast MC package and the properties of available detector descriptions can be found elsewhere [17].

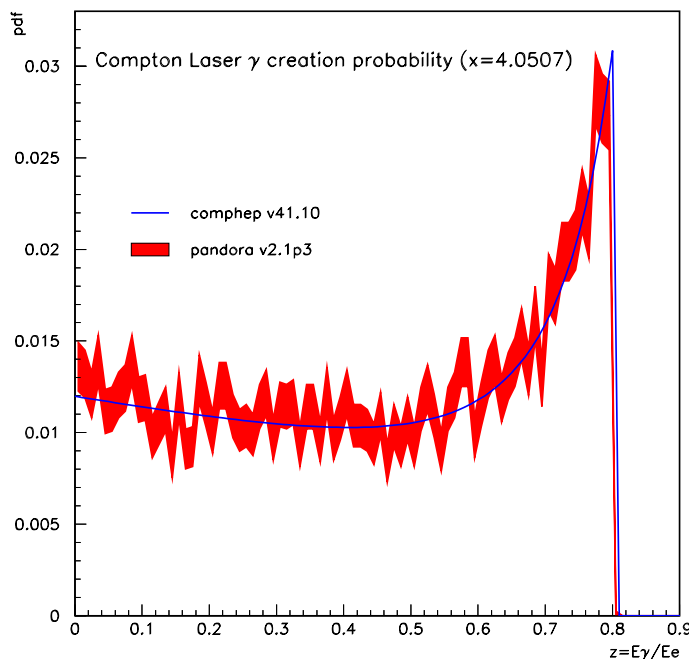


Figure 5. Laser spectra used in the two MC generators. The shaded band is the one sigma statistical error as computed in Pandora.

3. Event Selection

To find the appropriate cuts for each channel, 10,000 signal and 10,000 background events are generated and processed in the fast detector simulation [18]. For each channel, the appropriate cuts with their values are found by optimizing the statistical significance given by S/\sqrt{B} .

3.1. Lepton channels

In Table 1, signal and background effective cross sections ($\sigma \times Br$, after selection and generator level cuts) are given for leptonic decays of W , for \mathcal{E}_{ee} of 150 GeV. For W identification, the required signature is a

charged lepton (l) + \cancel{E}_T . So far only muon and electron channels are investigated. For both cases the particle identification is assumed to be 100% efficient.

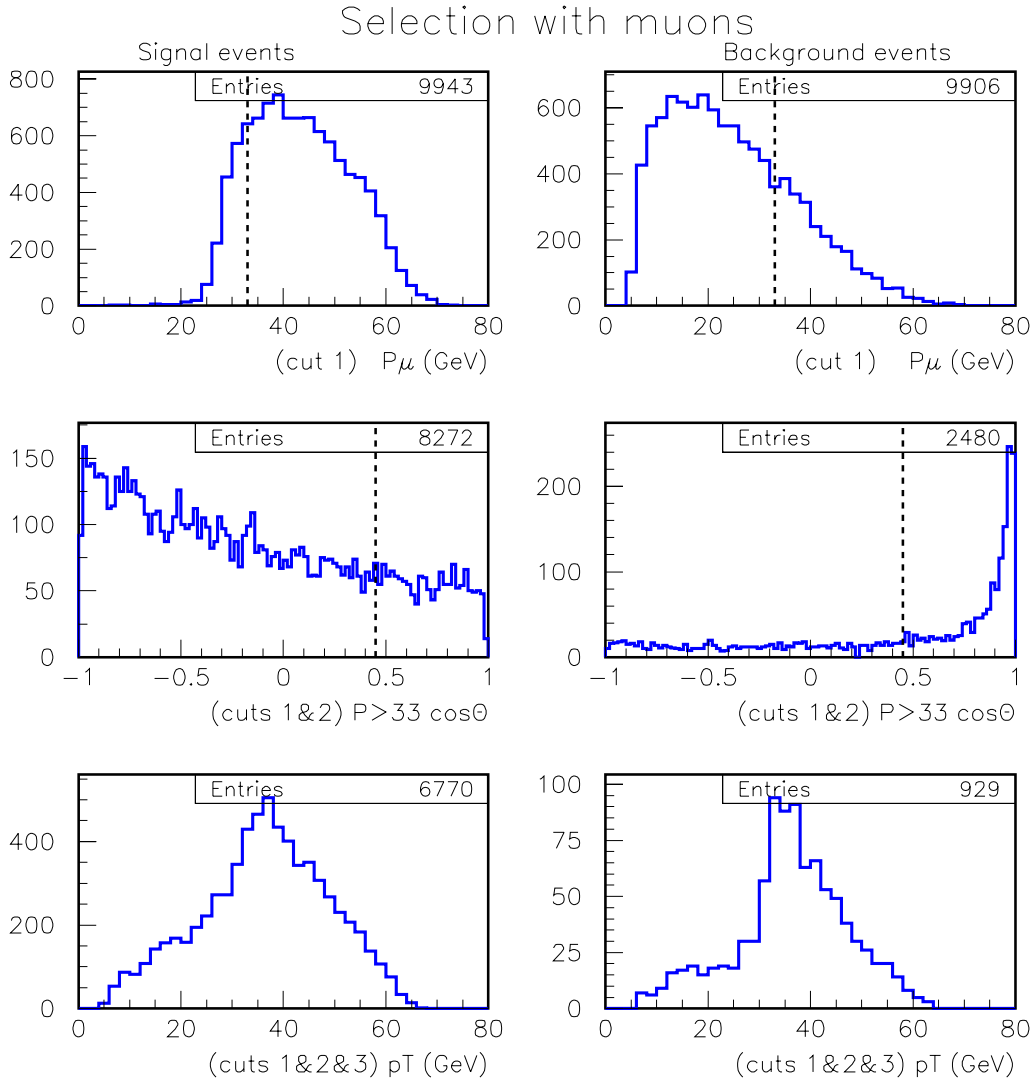


Figure 6. Kinematic distributions of signal (left column) and background (right column) muons. The dashed vertical lines represent the optimized cut values. The surviving background events having similar kinematic properties as the signal events, constitute an irreducible background.

The muons originating from the resolved photon are soft and they follow the direction of the initial photon. These two properties allow a reduction on the background of 91% for a signal loss of 32%. The applied cuts and their efficiencies are given in Table 2. Figure 6 shows the distributions of selected kinematic quantities for signal (left) and background (right) muons. The dashed vertical lines in the top four plots represent the optimized cut values. The two bottom plots are the transverse momenta of the remaining signal and background events. Given the similarity of these two distributions, we conclude that with the cuts applied in the analysis, this background is irreducible. The results of the similar studies for the electron channel are presented in Table 3.

3.2. Hadron channels

Final states containing $\bar{c}s$ and $\bar{u}d$ are the major contributors for both the signal and background cross sections. The contribution from the b quark is practically null due to the smallness of V_{cb} and V_{ub} . The

Table 2. With significance optimized cuts, 68% signal and 9% background events survive in the muon channel.

applied cut	signal loss (%)	background reduction (%)
No Jets, 1 Lepton	< 1	< 1
$P_\mu > 33$ GeV	17	75
$\cos(\Theta_\mu) < 0.45$	15	16

Table 3. With significance optimized cuts, 58% signal and 1% background events survive in the electron channel.

applied cut	signal loss (%)	background reduction (%)
No Jets, 1 Lepton	< 1	< 1
$P_e > 40$ GeV	42	99

jets are reconstructed with the DURHAM algorithm, with a typical rapidity cut y of 0.04. The required signature is a two jet event (2j) + \cancel{E}_T . Figure 7 contains distributions for selected quantities in solid gray for the signal and in hatched pattern for the backgrounds. The black dashed vertical lines show the selected cut values which were optimized by taking into account the fact that the background jets follow the initial photon direction with small transverse momenta. In each plot the additive effect of the selected cuts are presented. The optimized value for each cut and the cumulative efficiencies are also given in Table 4. With these cuts, about 90% of the background can be eliminated with a signal loss of about 50%. These ratios will be assumed to hold true for the other hadronic channels as well.

Table 4. With significance optimized cuts, 51% signal vs 9.6 background events survive in the $\bar{c}s$ channel.

applied cut	signal loss	background reduction
2 Jets only events	2.6%	7.4%
$\text{Cos}(\theta)$ both jets < 0.9	16%	45%
$P_{t_{jet}} > 11$ GeV	39%	80%
$53 < M_{inv,2jets} < 89$ GeV	49%	90.4%

4. Results and Conclusions

After the cuts, the effective cross section for the signal and background events in the muon and electron channels is given in Table 5. The error on the cross section is calculated with the number of events after background subtraction, assuming a Snowmass year of 10^7 seconds. The decrease of the statistical error in the signal cross section as a function of data taking time is shown in Figure 8 for electron and muon channels both separately and combined. If the events from two channels are combined, a measurement of \mathcal{P}_e with 1% statistical error can be obtained in less than a year of nominal operation with the Snowmass efficiency of about 30 percent.

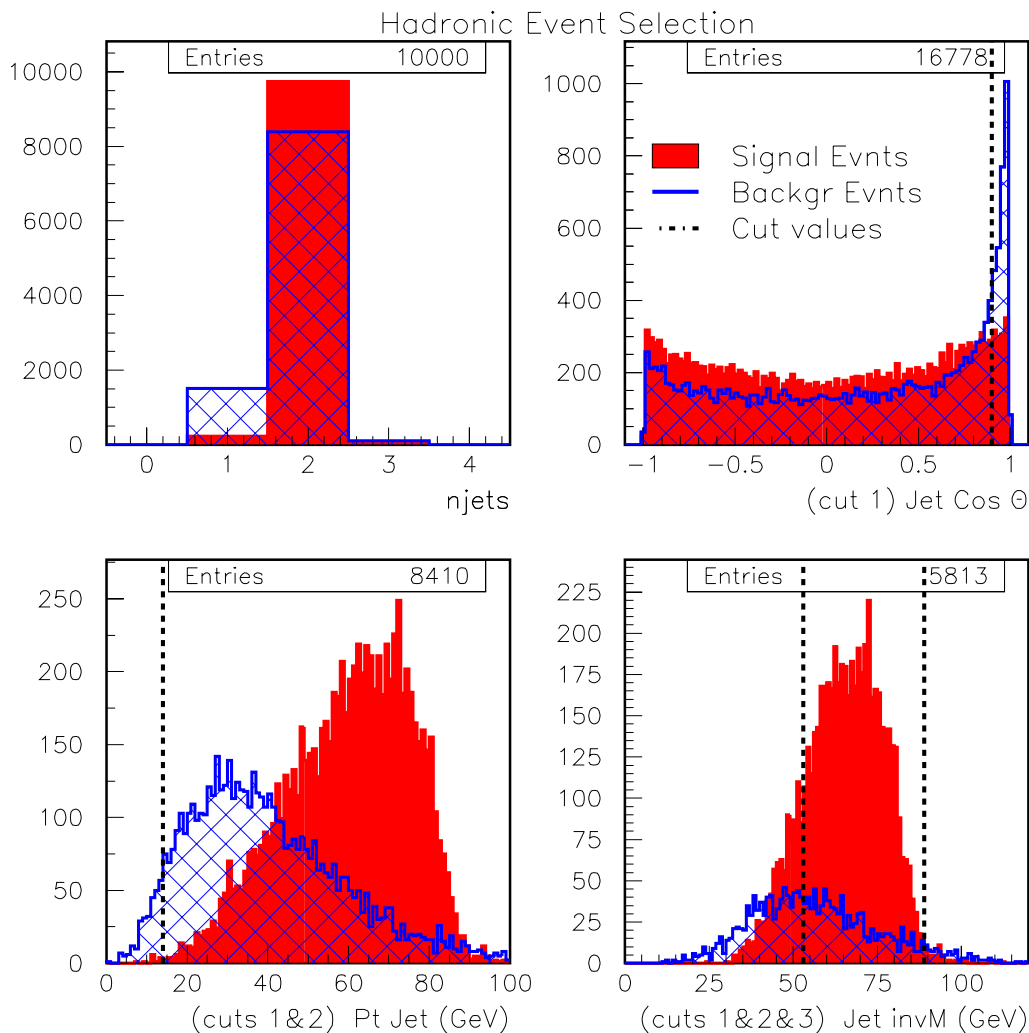


Figure 7. Hadronic signal (solid) and background (hatched) kinematic distributions. One of the two dominant channels, $\bar{c}s$, is shown as an example. The vertical dotted lines represent the the applied cut values.

Table 5. Effective σ s in fb in lepton channels.

μ	signal	background	e	signal	Z bg	γ bg
$\sigma_{eff}(fb)$	188.0	3.4	$\sigma_{eff}(fb)$	161.2	9.4	4.6

For the hadronic final states, only one subprocess was considered to find the optimal cuts. The obtained signal survival probability is then extended to all hadron channels to compute the total number of events necessary to make a precision measurement on the cross section. The effective cross sections of the signal and background processes after the applied cuts are shown in Table 6. The results of a precision measurement on the cross section to obtain the polarization is presented in Figure 9. We see that if the hadron channel is used, the polarization of the initial electron beam can be obtained with a one percent statistical error which can be obtained in about 3–4 months.

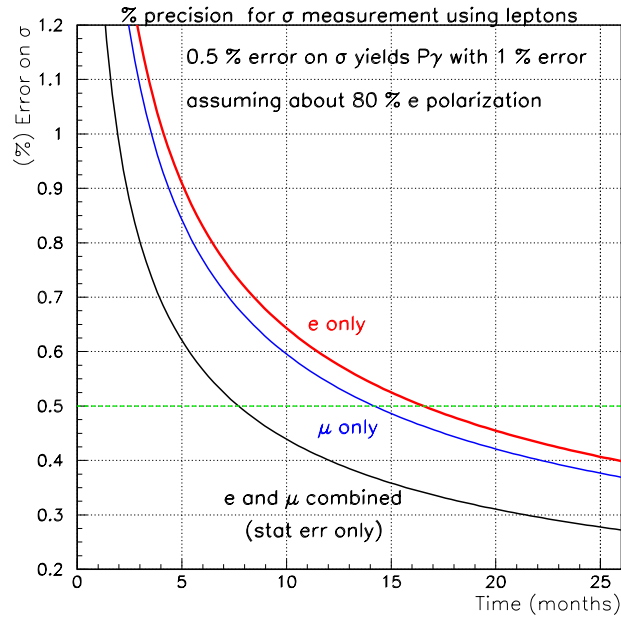


Figure 8. Precision on the cross section measurement with surviving signal events in leptonic channels is shown both separately and combined.

Table 6. Effective cross sections in fb for signal and background processes in the hadron channels.

qq'	signal	background
$\sigma_{eff}(fb)$	837	28

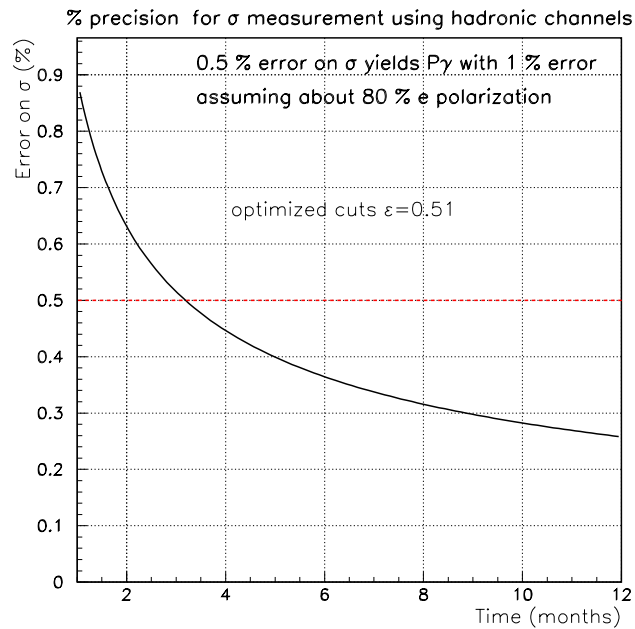


Figure 9. Precision on cross section measurement with surviving signal events using hadron channel.

For this study we have only considered the statistical errors and the direct backgrounds. The study of systematic errors coming from misidentifications and fakes is in progress. We conclude that it is feasible to measure the initial electron beam polarization with a good precision using the $e \gamma \rightarrow \nu W$ process.

Acknowledgments

The author is grateful to Mayda Velasco and Micheal Schmitt for introduction to the subject and to Müge Karagöz Ünel for fruitful discussions.

References

- [1] "Next Linear Collider (NLC) test accelerator: Conceptual design report", SLAC-0411, Aug 1993. 121pp.
"The CLIC Test Facility - CTF2: A Two beam test accelerator for linear collider studies ", CERN-PS-96-14-LP, Jun 1996. 40pp.
"TESLA linear collider: Status report ", LCWS 2000, Oct 2000.
- [2] T.W. Markiewicz and F. Pilat, Snowmass 2001 -Interaction Regions, Working group summary, J.Early, talk given at Linear Collider Workshop 2000,
R. Beach, talk given at NLC Workshop 2000
- [3] E.M. Gregores, M.C. Gonzalez-Garcia, S.F. Novaes, Phys.Rev. D56 (1997) 2920-2927
O. J. P. Eboli, J. K. Mizukoshi, Phys.Rev. D64 (2001) 075011
S. Atag and I Sahin, Phys.Rev. D64 (2001) 095002
- [4] O.J.P. Eboli et al, Phys.Lett. B311 (1993) 147-152
J.E. Cieza Montalvo, O.J.P. Eboli, Phys.Rev. D47 (1993) 837-843
- [5] D. Asner, et al, hep-ex/0111056, submitted to Eur. Phys. Jour.
- [6] DELPHI Collaboration, Phys.Lett. B502 (2001) 9-23
- [7] S. Godfrey et. al., Phys.Rev. D63 (2001) 053005
- [8] L. Jonsson, "Real and Virtual Photon Structure", Proceedings 'QCD and High Energy Hadronic Interactions', Recontres de Moriond, hep-ph/0207181.
- [9] M.E. Peskin, Talk given at 1999 International Workshop on Linear Colliders, hep-ph/9910519
- [10] T. Sjostrand, hep-ph/9508391
- [11] T. Abe, M. Iwasaki, Talk given at Snowmass 2001, hep-ex/0110068
- [12] A.Pukhov et al, hep-ph/9908288
- [13] A.S.Belyaev et al, Talk given at 7th International Workshop on Advanced Computing and Analysis Technics in Physics Research, (ACAT2000, Fermilab, October 16-20, 2000), hep-ph/0101232
- [14] C. Weizsaker, Z. Phys. 88, 612 (1934),
E.J. Williams, Phys. Rev. 45, 729 (1934)
- [15] V.I. Telnov, Nucl. Instr. Meth. A 294, (1990) 72.
- [16] L3 Collaboration, Phys.Lett. B517 (2001) 319-331
- [17] M. Iwasaki and T. Abe, Talk given at 5th International Linear Collider Workshop (LCWS2000), hep-ex/0102015
- [18] M. Iwasaki, Talk given at 4th International Linear Collider Workshop (LCWS1999), hep-ex/9910065